Supplementary Materials for

Targeting endogenous kidney regeneration using anti-IL11 therapy in acute and chronic models of kidney disease

Authors: Anissa A. Widjaja[1]*, Sivakumar Viswanathan[1], Shamini G. Shekeran[1], Eleonora Adami[1,2], Wei-Wen Lim[1,3], Sonia Chothani[1], Jessie Tan[3], Joyce Goh Wei Ting[1], Chen Hui Mei[1], Sze Yun Lim[1], Carine M Boustany-Kari[4], Julie Hawkins[4], Enrico Petretto[1], Norbert Hubner[2,5,6], Sebastian Schafer[1], Thomas M. Coffman[1], Stuart A. Cook[1,3,7]*

*Corresponding author. Email: anissa.widjaja@duke-nus.edu.sg and stuart.cook@duke-nus.edu.sg

This file includes:

Supplementary Figures (1-12)

Supplementary Table 1

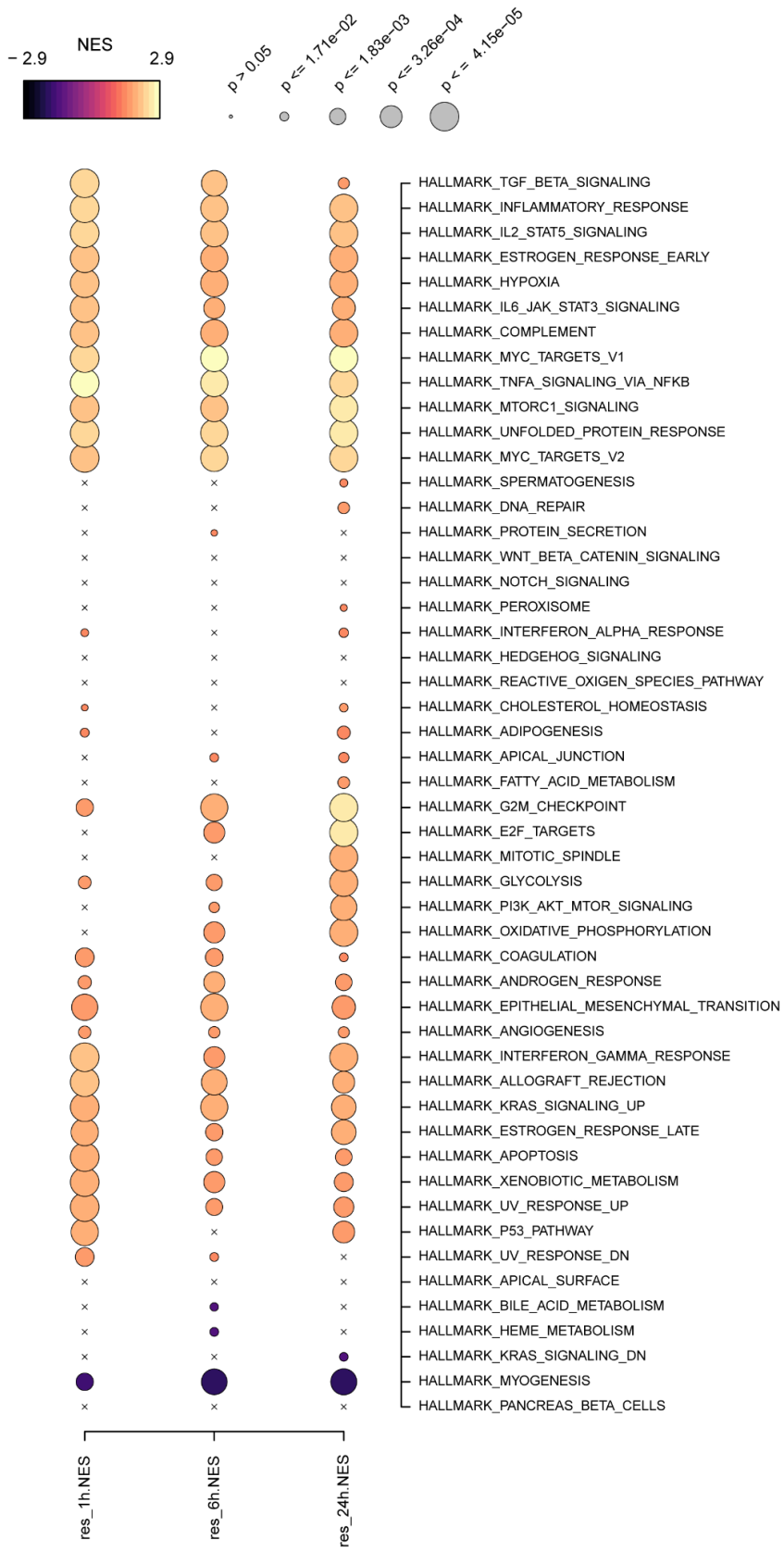
NES
− 2.9
2.9
p > 0.05
p <= 1.71e−02
p <= 1.83e−03
p <= 3.26e−04
p <= 4.15e−05
HALLMARK_TGF_BETA_SIGNALING
HALLMARK_INFLAMMATORY_RESPONSE
HALLMARK_IL2_STAT5_SIGNALING
HALLMARK_ESTROGEN_RESPONSE_EARLY
HALLMARK_HYPOXIA
HALLMARK_IL6_JAK_STAT3_SIGNALING
HALLMARK_COMPLEMENT
HALLMARK_MYC_TARGETS_V1
HALLMARK_TNFA_SIGNALING_VIA_NFKB
HALLMARK_MTORC1_SIGNALING
HALLMARK_UNFOLDED_PROTEIN_RESPONSE
HALLMARK_MYC_TARGETS_V2
HALLMARK_SPERMATOGENESIS
HALLMARK_DNA_REPAIR
HALLMARK_PROTEIN_SECRETION
HALLMARK_WNT_BETA_CATENIN_SIGNALING
HALLMARK_NOTCH_SIGNALING
HALLMARK_PEROXISOME
HALLMARK_INTERFERON_ALPHA_RESPONSE
HALLMARK_HEDGEHOG_SIGNALING
HALLMARK_REACTIVE_OXIGEN_SPECIES_PATHWAY
HALLMARK_CHOLESTEROL_HOMEOSTASIS
HALLMARK_ADIPOGENESIS
HALLMARK_APICAL_JUNCTION
HALLMARK_FATTY_ACID_METABOLISM
HALLMARK_G2M_CHECKPOINT
HALLMARK_E2F_TARGETS
HALLMARK_MITOTIC_SPINDLE
HALLMARK_GLYCOLYSIS
HALLMARK_PI3K_AKT_MTOR_SIGNALING
HALLMARK_OXIDATIVE_PHOSPHORYLATION
HALLMARK_COAGULATION
HALLMARK_ANDROGEN_RESPONSE
HALLMARK_EPITHELIAL_MESENCHYMAL_TRANSITION
HALLMARK_ANGIOGENESIS
HALLMARK_INTERFERON_GAMMA_RESPONSE
HALLMARK_ALLOGRAFT_REJECTION
HALLMARK_KRAS_SIGNALING_UP
HALLMARK_ESTROGEN_RESPONSE_LATE
HALLMARK_APOPTOSIS
HALLMARK_XENOBIOTIC_METABOLISM
HALLMARK_UV_RESPONSE_UP
HALLMARK_P53_PATHWAY
HALLMARK_UV_RESPONSE_DN
HALLMARK_APICAL_SURFACE
HALLMARK_BILE_ACID_METABOLISM
HALLMARK_HEME_METABOLISM
HALLMARK_KRAS_SIGNALING_DN
HALLMARK_MYOGENESIS
HALLMARK_PANCREAS_BETA_CELLS
res_1h.NES
res_6h.NES
res_24h.NES

Supplementary Figure 1: IL11 induces pro-inflammatory and epithelial-to-mesenchymal transcriptional responses in human tubular epithelial cells. Bubblemap showing results of hallmark gene set enrichment analysis for differentially expressed genes following IL11 stimulation over a time course (0, 1, 6, and 24 hours). Normalized enrichment scores for the hallmark gene sets were quantified using the fgsea R package with the fgsea-multilevel method that is based on an adaptive multilevel splitting Monte-Carlo approach. The quantified significance level was corrected using the Benjamini & Hochberg method. Normalized enrichment scores (NES) are represented by colors, from black (negative NES, suggesting down-regulation of the gene set) to yellow (positive NES, suggesting up-regulation). Dot size indicates significance, the larger the dot, the lower the adjusted p-value. Gene sets for the enrichment test were selected from the “H - Hallmark” collection in MSigDB. Source data are provided as a Source Data file.

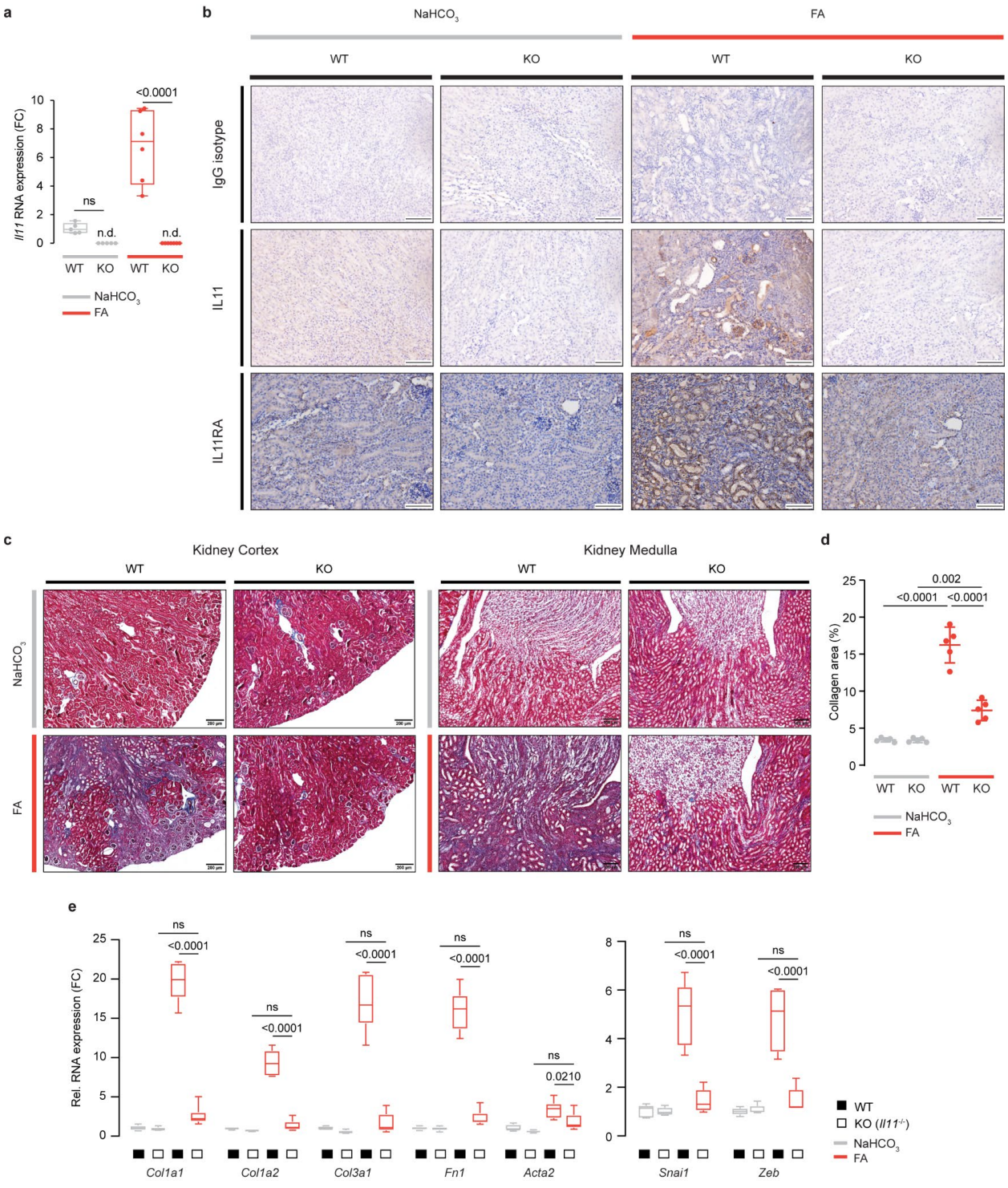

Supplementary Figure 2: *Il11* knockout mice are protected from renal inflammation and fibrosis. a Renal *Il11* RNA expression, **b** representative immunohistochemistry staining images of kidney stained for IL11 (with X203), IL11RA (with X209); staining with an IgG isotype control (11E10) is provided as negative control (representative dataset from n=3/group; scale bars: 100 µm), **c** representative Masson's Trichrome images of kidney cortex (scale bars: 200 µm) and medulla (scale bars: 100 µm) (representative dataset from n=5/group), **d** quantification of collagen area from Masson's Trichrome-stained kidney sections (n=5/group), **e** relative renal mRNA expression of fibrotic markers (*Col1a1, Col1a2, Col3a1, Fn1,*

Acta2), pro-inflammatory markers (*Tnfα*, *Il6, Ccl2*, *Ccl5, Il1β*), and pEMT markers (*Snai1*, and *Zeb*) from control and *Il11* KO mice post FA (Schematic Fig. 2a). **a, e** Data are shown as box-and-whisker with median (middle line), 25th–75th percentiles (box), and minimum-maximum values (whiskers); WT-$NaHC0_3$, $Il11^{-/-}$-$NaHC0_3$ (n=5/group), WT-FA (n=6), $Il11^{-/-}$-FA (n=7), **c** data are shown as mean±SD. **a, d, e** 2-way ANOVA with Sidak's correction. FC: Fold change. Source data are provided as a Source Data file.

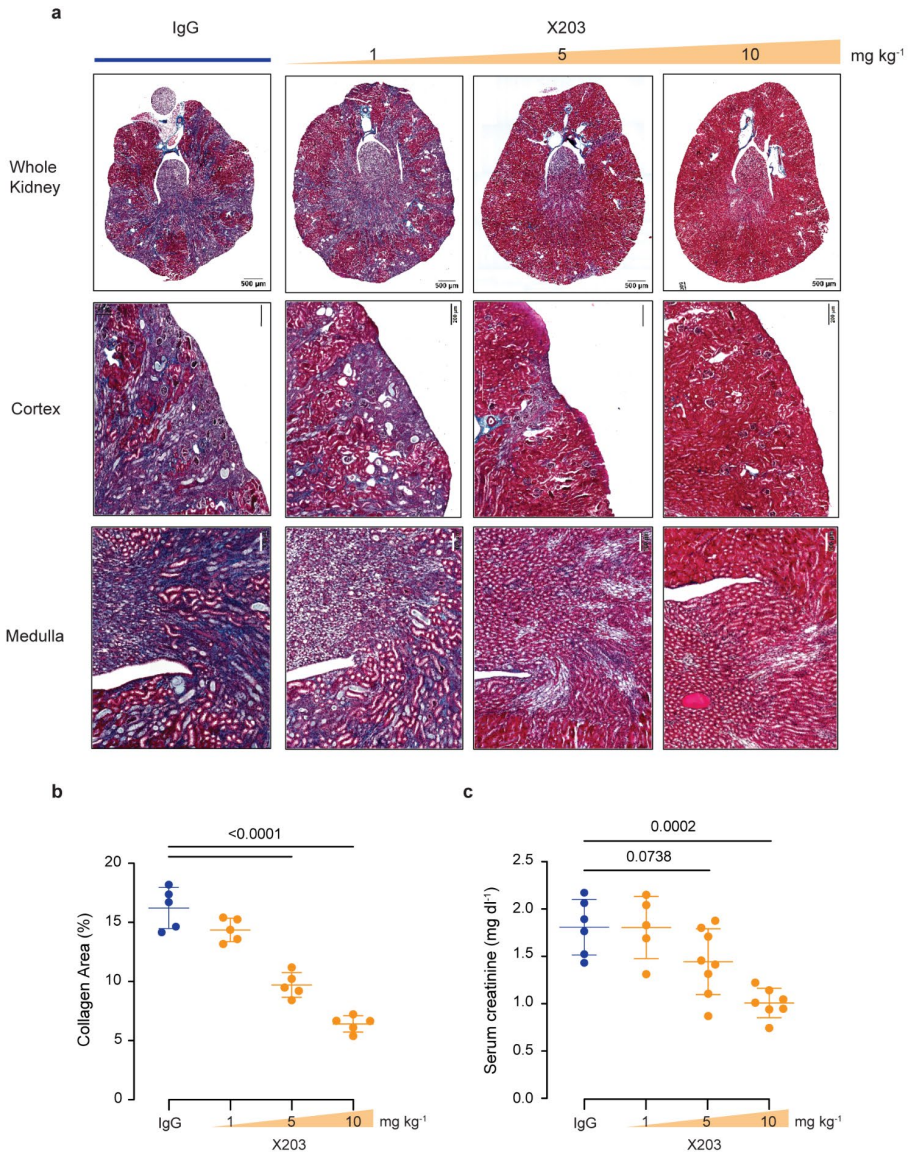

Supplementary Figure 3: Dose-dependent effects of anti-IL11 on renal fibrosis and function. a Representative Masson's Trichrome images of whole kidney cross section (scale bars: 500 µm), kidney cortex (scale bars: 200 µm), and kidney medulla (scale bars: 100 µm) (representative dataset from n=5/group), and **b** quantification of collagen area from Masson's Trichrome-stained kidney sections (n=5/group), **c** serum creatinine for X203 dose finding experiments, as compared to IgG (10 mg/kg), as represented in Schematic Fig. 3a (IgG (n=6), X203 1 mg/kg (n=5), X203 5 mg/kg (n=8), X203 10 mg/kg (n=7)). **b**, **c** Data are shown as mean±SD, one-way ANOVA with Dunnett's correction. Source data are provided as a Source Data file.

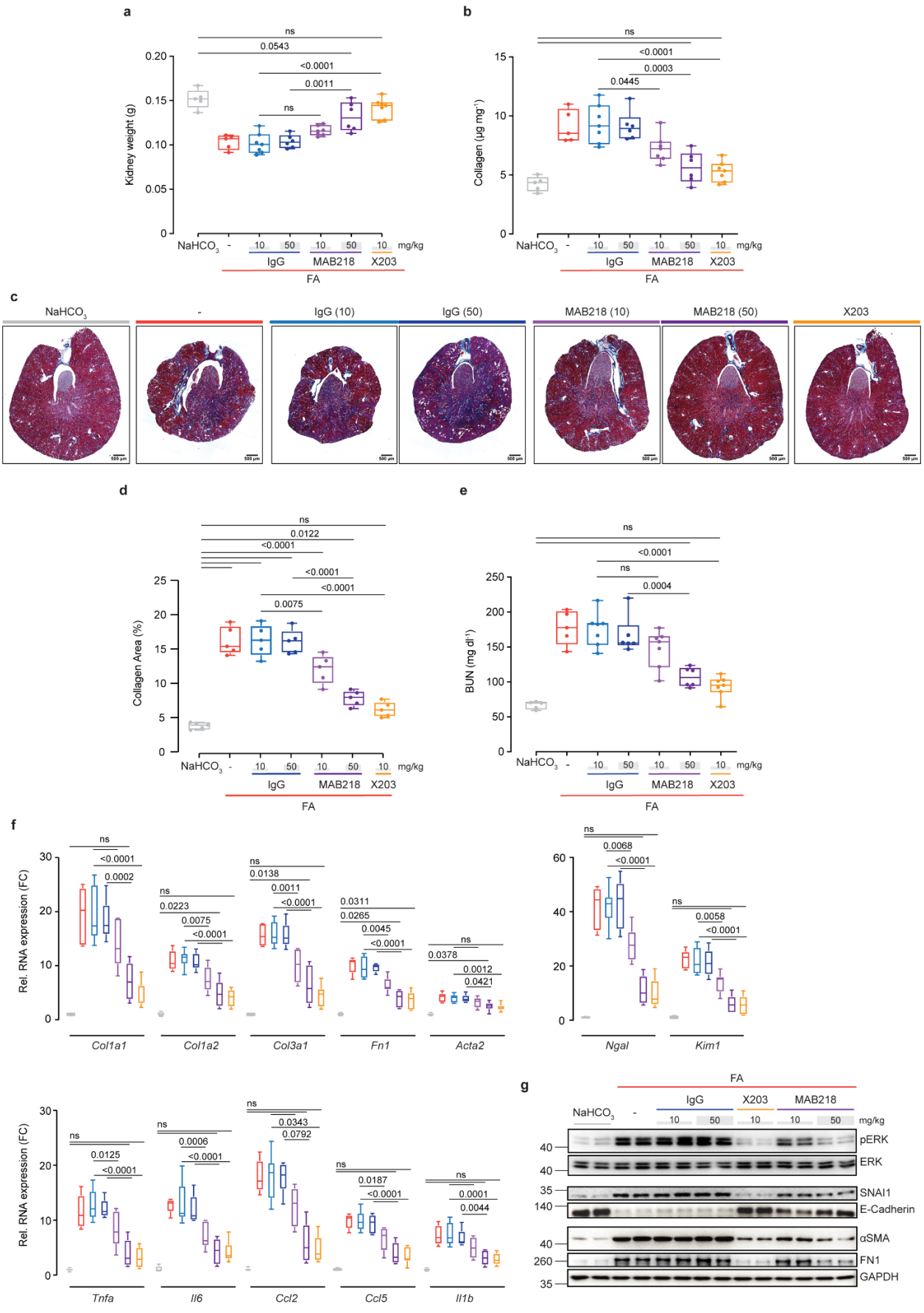
a
Kidney weight (g)
ns
0.0543
<0.0001
0.0011
ns
NaHCO3 - 10 50 10 50 10 mg/kg
IgG MAB218 X203
FA
b
Collagen (µg mg-1)
ns
<0.0001
0.0003
0.0445
NaHCO3 - 10 50 10 50 10 mg/kg
IgG MAB218 X203
FA
c
NaHCO3
-
IgG (10)
IgG (50)
MAB218 (10)
MAB218 (50)
X203
d
Collagen Area (%)
ns
0.0122
<0.0001
<0.0001
<0.0001
0.0075
NaHCO3 - 10 50 10 50 10 mg/kg
IgG MAB218 X203
FA
e
BUN (mg dl-1)
ns
<0.0001
ns
0.0004
NaHCO3 - 10 50 10 50 10 mg/kg
IgG MAB218 X203
FA
f
Rel. RNA expression (FC)
Col1a1
Col1a2
Col3a1
Fn1
Acta2
Ngal
Kim1
Tnfa
Il6
Ccl2
Ccl5
Il1b
g
FA
IgG X203 MAB218
NaHCO3 - 10 50 10 10 50 mg/kg
pERK
ERK
SNAI1
E-Cadherin
αSMA
FN1
GAPDH

Supplementary Figure 4: Therapeutic effects of two separate IL11 neutralizing antibodies (X203 and MAB218) on renal phenotypes following folic acid-induced nephrotoxicity. a Kidney weight, **b** kidney collagen content by hydroxyproline assay, **c** representative Masson's Trichrome images of whole kidney cross section (scale bars: 500 µm, representative dataset from n=5/group), **d** quantification of collagen area from Masson's Trichrome-stained kidney sections (n=5/group), **e** BUN, **f** relative renal mRNA expression of *Col1a1*, *Col1a2*, *Col3a1*, *Fn1*, *Acta2, Ngal, Kim1*,*Tnfα*, *Il6, Ccl2*, *Ccl5*, and *Il1β* (n=5-7/group), and **g** Western blots of pERK, ERK, SNAI1, E-Cadherin, αSMA, Fibronectin, and GAPDH (representative dataset from n=5/group) for X203 and MAB218 therapeutic comparison experiments as shown in Schematic Fig. 3d. **a, b, e, f** $NaHC0_3$, FA (n=5/group), IgG/MAB218/X203 (10 mg/kg) (n=7/group), IgG/MAB218 (50 mg/kg) (n=6/group). **a, b, d-f** Data are shown as box-and-whisker with median (middle line), 25th–75th percentiles (box), and minimum-maximum values (whiskers), one-way ANOVA with Tukey's correction except for (**f**, *Ccl2*) which was analyzed by Kruskal-Wallis with Dunn's correction. Source data are provided as a Source Data file.

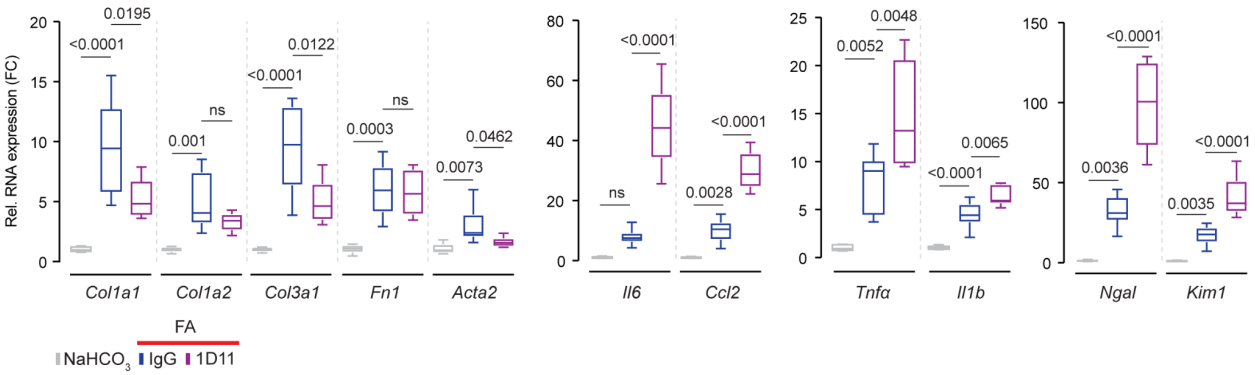

Supplementary Figure 5: Markers of fibrosis, inflammation, and kidney damage in injured kidneys of mice receiving anti-TGFβ (1D11) treatment. Relative renal mRNA expression levels of fibrosis (*Col1a1, Col1a2, Col3a1, Fn1, Acta2),* pro-inflammatory (*Tnfα*, *Il6, Ccl2*, *Il1β*), and kidney injury (*Ngal*, *Kim1*) markers for experiments illustrated in Schematic Fig. 3f ($NaHC0_3$ (n=4), FA+IgG (n=10), FA+1D11 (n=6). Data are shown as box-and-whisker with median (middle line), 25th–75th percentiles (box), and minimum-maximum values (whiskers), one-way ANOVA with Tukey's correction. Source data are provided as a Source Data file.

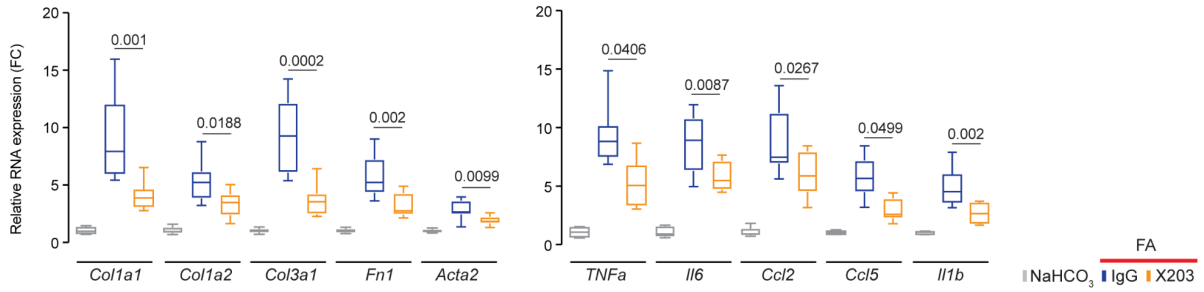

Supplementary Figure 6: Markers of fibrosis and inflammation in the kidneys of mice subjected to folic acid induced renal injury and given X203 in a treatment mode. Relative renal mRNA expression of *Tnfα*, *Il6, Ccl2*, *Ccl5*, *Il1β*, *Col1a1*, *Col1a2*, *Col3a1*, *Fn1*, and *Acta2* for X203 therapeutic dosing experiments as illustrated in Schematic Fig. 4a ($NaHC0_3$ (n=5), FA+IgG (n=9), FA+X203 (n=8)). Data are shown as box-and-whisker with median (middle line), 25th–75th percentiles (box), and minimum-maximum values (whiskers), one-way ANOVA with Tukey's correction except for (*Tnfα*, *Ccl5*) which were analyzed by Kruskal-Wallis with Dunn's correction. Source data are provided as a Source Data file.

.

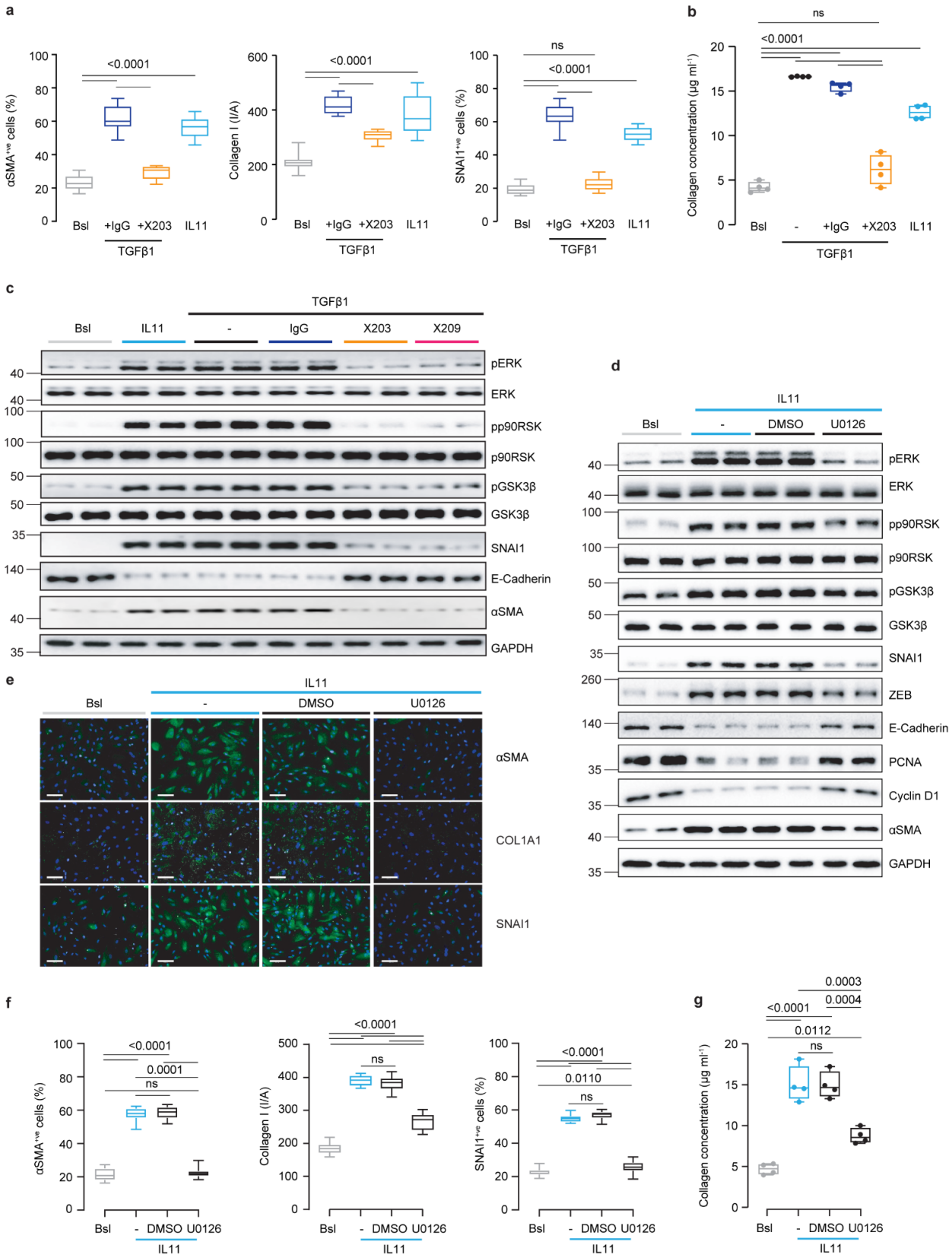
a
αSMA+ve cells (%)
<0.0001
Bsl
+IgG
+X203
IL11
TGFβ1
Collagen I (I/A)
<0.0001
SNAI1+ve cells (%)
ns
<0.0001
b
Collagen concentration (μg ml-1)
ns
<0.0001
Bsl
-
+IgG
+X203
IL11
TGFβ1
c
TGFβ1
Bsl
IL11
-
IgG
X203
X209
pERK
ERK
pp90RSK
p90RSK
pGSK3β
GSK3β
SNAI1
E-Cadherin
αSMA
GAPDH
d
IL11
Bsl
-
DMSO
U0126
pERK
ERK
pp90RSK
p90RSK
pGSK3β
GSK3β
SNAI1
ZEB
E-Cadherin
PCNA
Cyclin D1
αSMA
GAPDH
e
IL11
Bsl
-
DMSO
U0126
αSMA
COL1A1
SNAI1
f
αSMA+ve cells (%)
<0.0001
0.0001
ns
Collagen I (I/A)
<0.0001
ns
SNAI1+ve cells (%)
<0.0001
0.0110
ns
Bsl
-
DMSO
U0126
IL11
g
Collagen concentration (μg ml-1)
0.0003
0.0004
<0.0001
0.0112
ns
Bsl
-
DMSO
U0126
IL11

Supplementary Figure 7: X203 inhibits TEC mesenchymal transition in an ERK dependent manner. **a** Quantification of αSMA^{+ve} and SNAI1^{+ve} cells and Collagen 1 immunostaining (n=14/group) and **b** collagen secretion in the supernatant (n=4/group) from TECs stimulated with either IL11 or TGFβ in the presence of IgG/X203. **c** Western blots of pERK, ERK, pp90RSK, p90RSK, pGSK3β, GSK3β, SNAI1, E-Cadherin, and GAPDH for TECs stimulated with either IL11 or TGFβ in the presence of IgG, X203 (anti-IL11), or X209 (anti-IL11RA) (representative dataset from n=4/group). **d** Western blots of pERK, ERK, pp90RSK, p90RSK, pGSK3β, GSK3β, SNAI1, ZEB, E-Cadherin, PCNA, Cyclin D1, αSMA, and GAPDH (representative dataset from n=4/group), **e** representative IF images (scale bars: 100 µm, representative dataset from n=3/group) and **f** quantification of αSMA^{+ve} and SNAI1^{+ve} cells (n=14/group) and Collagen 1 immunostaining (n=21/group) for TECs stimulated with IL11 alone or in the presence of either DMSO or U0126. **g** Collagen secretion in the supernatant (n=4/group) from bsl, IL11, IL11+DMSO, and IL 11+U0126 group. **a-g** IL11 (5 ng/ml), TGFβ1 (5 ng/ml), IgG/X203/X209 (2 µg/ml), U0126 (10 µM); 24-hour stimulation. **a, b, f, g** Data are shown as box-and-whisker with median (middle line), 25th–75th percentiles (box), and minimum-maximum values (whiskers), one-way ANOVA with Tukey's correction (except for F, αSMA^{+ve} which was analyzed by Kruskal-Wallis with Dunn's correction). Bsl: Baseline; I/A: Intensity/Area. Source data are provided as a Source Data file.

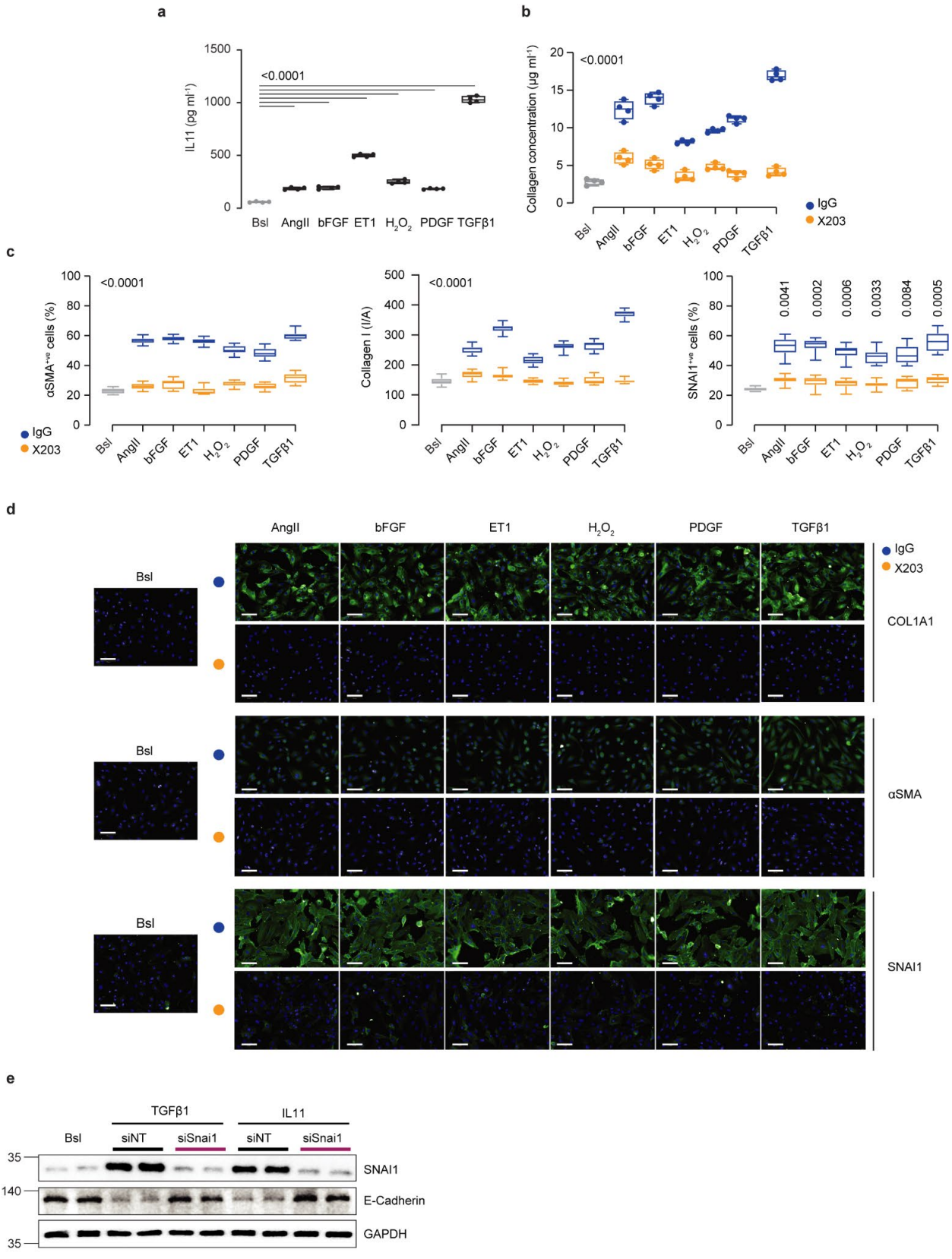
a
IL11 (pg ml-1)
<0.0001
Bsl AngII bFGF ET1 H2O2 PDGF TGFβ1
b
Collagen concentration (μg ml-1)
<0.0001
IgG
X203
c
αSMA+ve cells (%)
Collagen I (I/A)
SNAI1+ve cells (%)
0.0041 0.0002 0.0006 0.0033 0.0084 0.0005
d
AngII bFGF ET1 H2O2 PDGF TGFβ1
Bsl
COL1A1
αSMA
SNAI1
e
TGFβ1
IL11
siNT
siSnai1
35
140
SNAI1
E-Cadherin
GAPDH

Supplementary Figure 8: IL11 signaling is required for induction of pEMT in TECs. **a** ELISA of secreted IL11 (n=4/group), **b** the amount of secreted collagen in the supernatant (n=4/group), **c** quantification (n=14/group), and **d** representative IF images (scale bars: 100 µm, representative dataset from n=3/group) of αSMA^{+ve} and SNAI1^{+ve} cells and Collagen 1 immunostaining from TECs after 24-hour treatment with Angiontensin II (AngII), basic FGF (bFGF), Endothelin-1 (ET-1), H_20_2, PDGF, and TGFβ. **e** Western blots of SNAI1, E-Cadherin, and GAPDH from TECs stimulated with TGFβ or IL11 subjected to siRNA knockdown for SNAI1 (NT: non targeting siRNA control) (representative dataset from n=4/group). **a-e** TGFβ1 (5 ng/ml), IL11 (5 ng/ml), AngII (100 nM), bFGF (10 ng/ml), Endothelin 1 (ET-1, 250 ng/ml), H_20_2 (0.2 mM), PDGF (20 ng/ml), IgG/X203/(2 µg/ml), siNT/siSNAI1 (25 nM); 24-hour stimulation. **a-c** Data are shown as box-and-whisker with median (middle line), 25th–75th percentiles (box), and minimum-maximum values (whiskers). **a** One-way ANOVA with Dunnett's correction; **b,c** one-way ANOVA with Tukey's correction (except for C, SNAI1^{+ve} which was analyzed by Kruskal-Wallis with Dunn's correction). Bsl: Baseline; I/A: Intensity/Area. Source data are provided as a Source Data file.

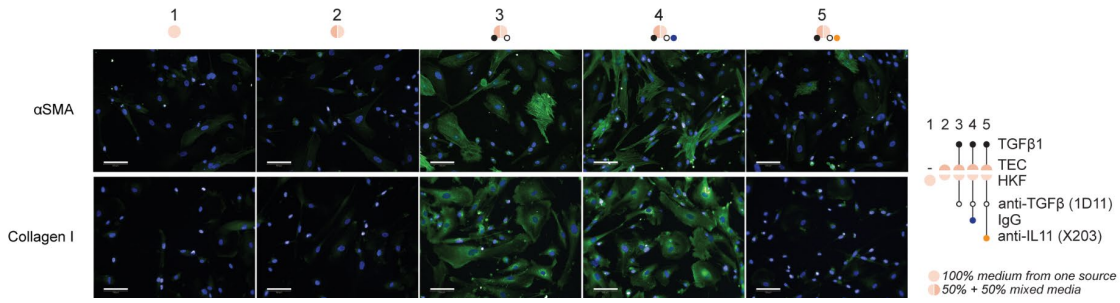

Supplementary Figure 9: Paracrine IL11 (but not TGFβ) activity from TECs causes renal fibroblast-to-myofibroblast transition. Representative images (scale bars: 100 μm, representative dataset from n=3/group) of αSMA^{+ve} cells and Collagen 1 immunostaining from media transfer experiments in which conditioned media from control or TGFβ-stimulated TECs (24 hours) were used to treat primary human kidney fibroblasts (HKFs) in the presence of anti-TGFβ (1D11) alone or with either IgG or X203 as shown by the schematic on the right. Source data are provided as a Source Data file.

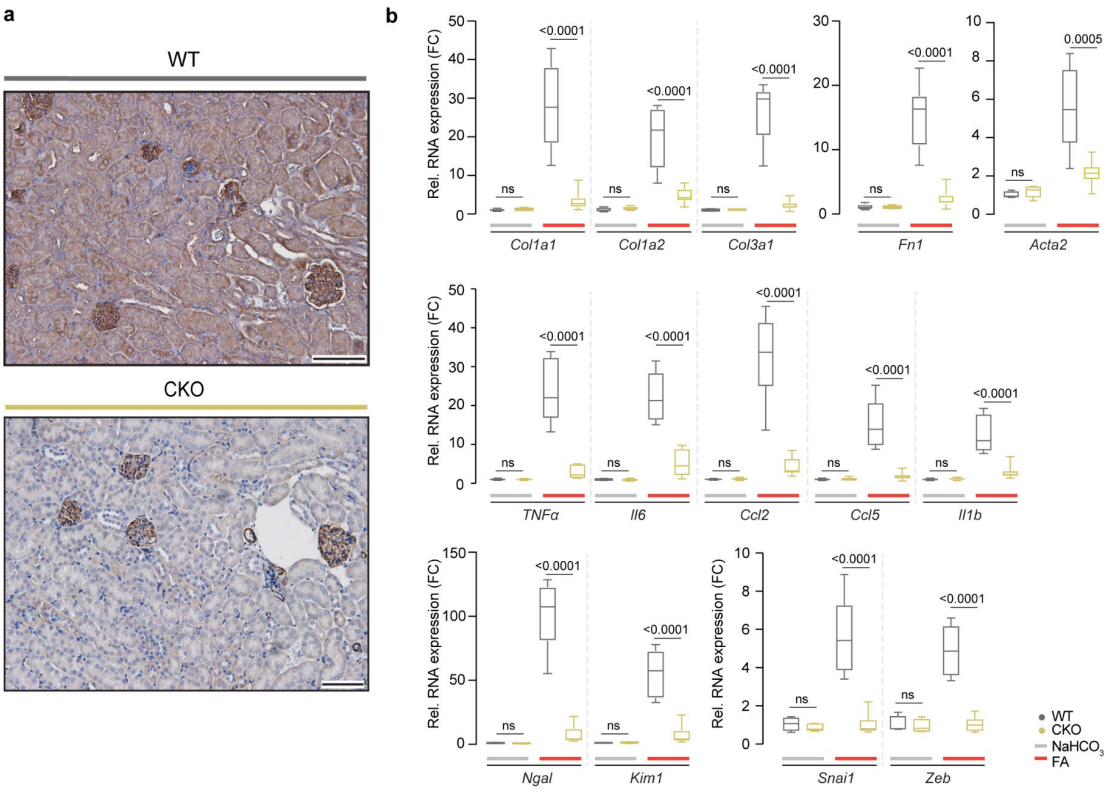

Supplementary Figure 10: Mice with TEC-specific *Il11ra1* deletion are protected from fibrosis, inflammation and tubule damage following AKI. a Representative immunohistochemistry images of IL11RA staining in kidneys from wild-type (WT) and TEC-specific *Il11ra1*-deleted (CKO) mice (scale bars: 100 µm; representative dataset from n=3/group). **b** Relative renal mRNA expression levels of fibrotic markers (*Col1a1, Col1a2, Col3a1, Fn1, Acta2),* kidney injury markers (*Ngal*, *Kim1*), pro-inflammatory markers (*Tnfα*, *Il6, Ccl2*, *Ccl5, Il1β*), and pEMT markers (*Snai1*, *Zeb*) for experiments shown in Schematic Fig. 7a (WT-$NaHC0_3$ (n=4), CKO-$NaHC0_3$ (n=5), WT-FA (n=8), CKO-FA (n=7)). Data are shown as box-and-whisker with median (middle line), 25th–75th percentiles (box), and minimum-maximum values (whiskers), 2-way ANOVA with Sidak's correction. Source data are provided as a Source Data file.

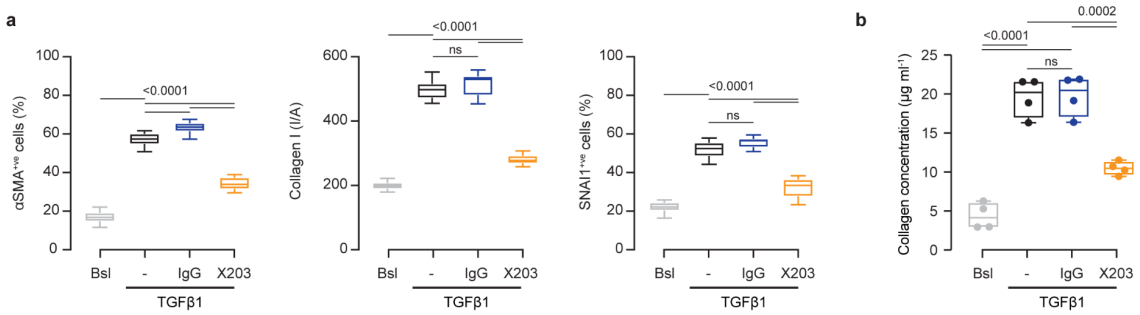

Supplementary Figure 11: Inhibition of IL11 signaling reverts TECs that were in mesenchymal state back to an epithelial phenotype. Quantification of **a** αSMA^{+ve} and SNAI1^{+ve} cells and Collagen 1 immunostaining (n=14/group), and **b** collagen secretion in the supernatant from TEC reversal experiments as shown in Schematic Fig. 6a. Data are shown as box-and-whisker with median (middle line), 25th–75th percentiles (box), and minimum-maximum values (whiskers), one-way ANOVA with Tukey's correction. Source data are provided as a Source Data file.

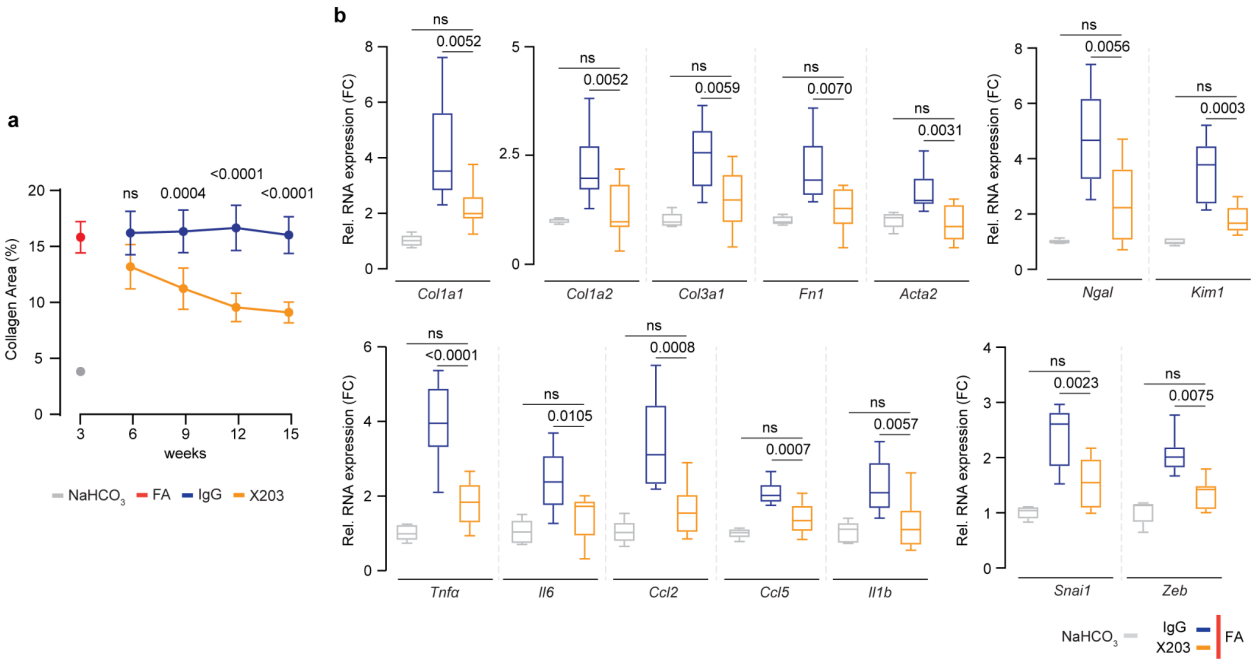

Supplementary Figure 12: X203 reverses pEMT-driven renal fibrosis, inflammation, and parenchymal damage in mice with chronic kidney disease. a Quantification of collagen area from Masson's Trichrome-stained kidney sections (n=4/group for kidneys collected at week 6, 9, and , n=5/group from those collected at other time points). Data are shown as mean ± SD; 2-way ANOVA with Sidak's correction. **b** Relative renal mRNA expression levels of fibrotic markers (*Col1a1, Col1a2, Col3a1, Fn1, Acta2),* kidney injury markers (*Ngal*, *Kim1*), pro-inflammatory markers (*Tnfα*, *Il6, Ccl2*, *Ccl5, Il1β*), and pEMT markers (*Snai1*, *Zeb*) for experiments shown in Schematic Fig. 9a ($NaHC0_3$ (n=5), FA FA+IgG/X203 (W15) (n=9/group)). Data are shown as box-and-whisker with median (middle line), 25th–75th percentiles (box), and minimum-maximum values (whiskers), one-way ANOVA with Tukey's correction (except for *Zeb* which was analyzed by Kruskal-Wallis with Dunn's correction). Source data are provided as a Source Data file.

Supplementary Table 1: SYBR primer sequences for qPCR

Host	Gene	Forward (5'-3')	Reverse (5'-3')
Mouse	***Acta2***	TCCATCGTCCACCGCAAAT	GCCAGGGCTACAAGTTAAGG
	Ccl2	GAAGGAATGGGTCCAGACAT	ACGGGTCAACTTCACATTCA
	Ccl5	GCTGCTTTGCCTACCTCTCC	TCGAGTGACAAACACGACTGC
	Col1a1	GAGCAGACGGGAGTTTCTCCT	CATGTAGACTCTTTGCGGCTG
	Col1a2	AGGATTGGTCAGAGCAGTGT	TCCACAACAGGTGTCAGGGT
	Col3a1	CCACCCAATACAGGTCAAATGC	TGAGTATGACCGTTGCTCTGC
	Gapdh	CTGGAAAGCTGTGGCGTGAT	GACGGACACATTGGGGGTAG
	Il1β	CACAGCAGCACATCAACAAG	GTGCTCATGTCCTCATCCTG
	Kim1	AAACCAGAGATTCCCACACG	GTCGTGGGTCTTCCTGTAGC
	Ngal	TGGCCCTGAGTGTCATGTG	CTCTTGTAGCTCATAGATGGTGC
	Tnfα	ATGAGAAGTTCCCAAATGGC	CTCCACTTGGTGGTTTGCTA
	Snai1	CACACGCTGCCTTGTGTCT	GGTCAGCAAAAGCACGGTT
	Zeb	GCTGGCAAGACAACGTGAAAG	GCCTCAGGATAAATGACGGC
Human	***DUSP5***	GCCAGCTTATGACCAGGGTG	GTCCGTCGGGAGACATTCAG

Uncropped blots for supplementary figures

Supplementary Figure 4g

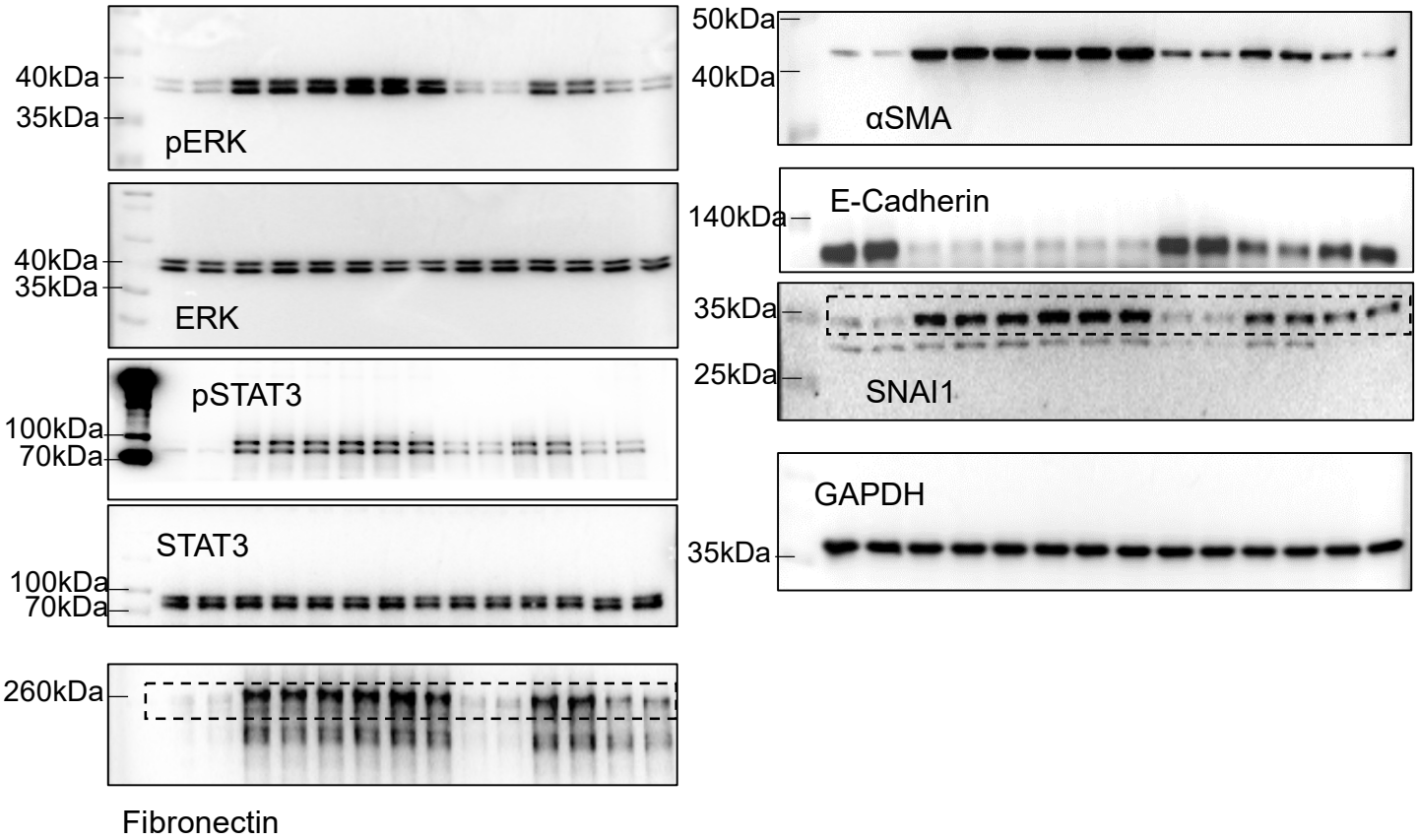

Supplementary Figure 7c

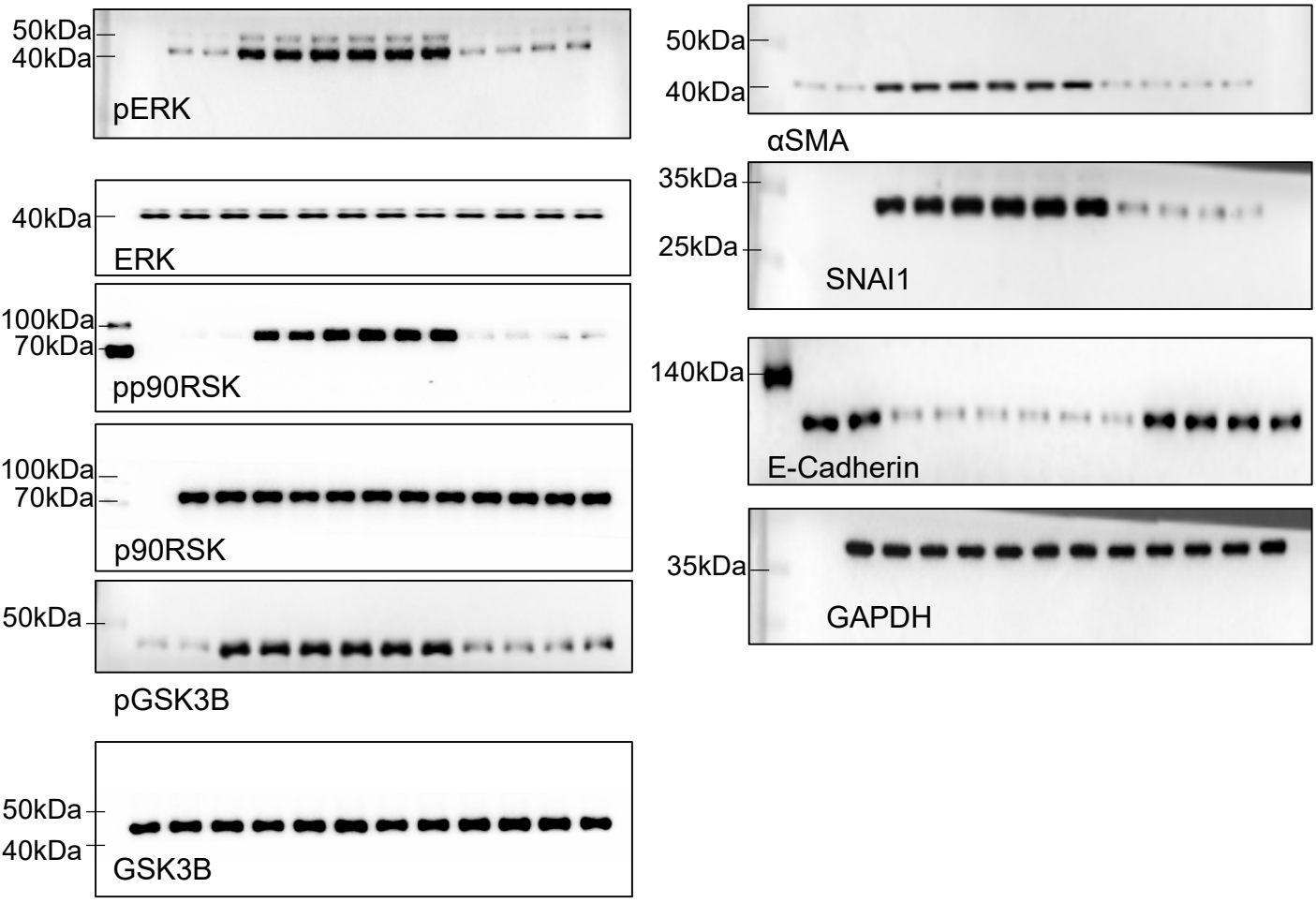

Supplementary Figure 7d

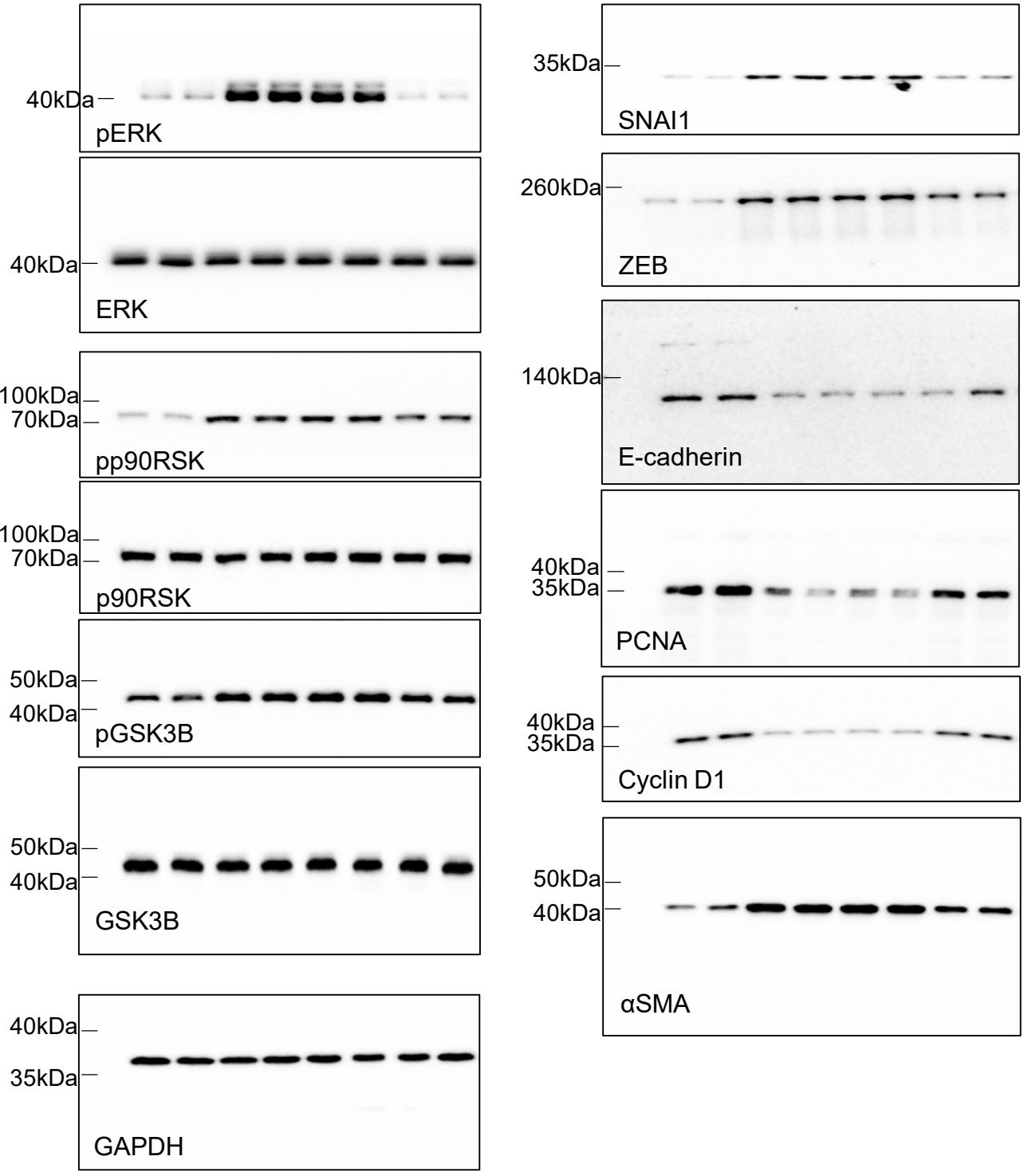

Supplementary 8e